ACCELERATED COMMUNICATION

THE JOURNAL OF BIOLOGICAL CHEMISTRY VOL. 291, NO. 42, pp. 21848–21856, October 14, 2016

Metformin Improves Metabolic Memory in High Fat Diet (HFD)-induced Renal Dysfunction*[S]◆

Received for publication, April 15, 2016, and in revised form, August 4, 2016
Published, JBC Papers in Press, August 22, 2016, DOI 10.1074/jbc.C116.732990

Kulbhushan Tikoo[1,2], Ekta Sharma[1], Venkateswara Rao Amara[1], Himani Pamulapati, and Vaibhav Shrirang Dhawale

From the Laboratory of Epigenetics and Diseases, Department of Pharmacology and Toxicology, National Institute of Pharmaceutical Education and Research, S.A.S. Nagar (Mohali), Punjab-160062, India

Recently, we have shown that high fat diet (HFD) *in vivo* and *in vitro* generates metabolic memory by altering H3K36me2 and H3K27me3 on the promoter of *FOXO1* (transcription factor of gluconeogenic genes) (Kumar, S., Pamulapati, H., and Tikoo, K. (2016) *Mol. Cell. Endocrinol.* 422, 233–242). Here we checked the hypothesis whether concomitant diet reversal and metformin could overcome HFD-induced metabolic memory and renal damage. Male adult Sprague-Dawley rats were rendered insulin-resistant by feeding high fat diet for 16 weeks. Then the rats were subjected to diet reversal alone and along with metformin for 8 weeks. Biochemical and histological markers of insulin resistance and kidney function were measured. Blood pressure and *in vivo* vascular reactivity to angiotensin II (200 mg kg^{-1}) were also checked. Diet reversal could improve lipid profile but could not prevent renal complications induced by HFD. Interestingly, metformin along with diet reversal restored the levels of blood glucose, triglycerides, cholesterol, blood urea nitrogen, and creatinine. In kidney, metformin increased the activation of AMP-activated protein kinase (AMPK) and decreased inflammatory markers (COX-2 and IL-1β) and apoptotic markers (poly(ADP-ribose) polymerase (PARP) and caspase 3). Metformin was effective in lowering elevated basal blood pressure and acute change in mean arterial pressure in response to angiotensin II (Ang II). It also attenuated tubulointerstitial fibrosis and glomerulosclerosis induced by HFD feeding in kidney. Here we report, for the first time, that metformin treatment overcomes metabolic memory and prevents HFD-induced renal damage.

Long-term prospective clinical studies, the Diabetes Control and Complications Trial (DCCT), the follow-up study Epidemiology of Diabetes Interventions and Complications (EDIC), and the United Kingdom Prospective Diabetes Study (UKPDS), stated that benefits of strict glycemic control following a period of poor glycemic control cannot be harnessed immediately following a period of poor glycemic control (1). This was called "metabolic or hyperglycemic memory" by the former two studies and "legacy effect" by the latter.

Various mechanisms have been used to explain the underlying cause of metabolic memory. There is a well established temporal relationship between the duration of poor glycemia and incidence of long-term complications. Glucotoxicity induces some irreversible mitochondrial or vascular changes, which then proceed to overt long-term complications. They also cause long-lasting activation of epigenetic changes in the promoter region of key inflammatory mediators as depicted in mice (2). Short-term hyperglycemia induces long-term changes in chromatin modifications (3). Poor glycemic control is associated with elevated oxidative stress and advanced glycation end products, which damage mitochondrial DNA in kidney, which in turn accentuates the risk of cardiovascular diseases (4). Dysregulated polyols, hexosamine fluxes, and activation of PKC isoforms induced by hyperglycemia also mediate renal damage (2).

Insulin resistance arises because of many reasons, such as increased Ser/Thr phosphorylation (rather than Tyr phosphorylation) of insulin receptor substrate (IRS) proteins, increased activity of Tyr phosphatases (*e.g.* SHIP2, phosphatase and tensin homolog (PTEN), and PTP-1B), and decreased activation of insulin receptor downstream signaling molecules (*e.g.* AKT, atypical PKC, etc.) (5). Chronic consumption of high fat diet leads to elevated levels of non-essential free fatty acids such as palmitic acid. In a series of classical experiments, Randle *et al.* (6) showed that fatty acids compete with glucose for substrate oxidation and hypothesized that increased fat oxidation is responsible for insulin resistance in obesity (reviewed in Ref. 7). Insulin resistance develops in type 2 diabetes and lipodystrophy because of the alteration in the partitioning of fat between the adipocyte and muscle or liver. This leads to the intracellular accumulation of triglycerides and fatty acid metabolites (diacylglycerol, ceramides, fatty acyl CoAs, etc.) in insulin-responsive tissues, leading to insulin resistance (8).

Insulin resistance and hyperinsulinemia due to the adipocytokine-induced activation of IκB kinase (IKK), JNK, and PKC create an imbalance between PI3K/Akt and MAPK axes, decrease NO-dependent vasodilation, and increase vasoreactivity and angiogenesis, which are known to promote kidney dysfunction. A growing body of preclinical data suggests that glomerular hypertrophy appears within the period of hyperinsulinemia itself, before the onset of overt diabetes (2, 9). Profibrotic TGF-β damages glomerular function by overproduction of interstitial tissue matrix, thickening of the glomerular basement membrane, and the down-regulation of matrix metalloproteinase (MMP)-2, an enzyme involved in matrix degradation, eventually ending in albumin leakage into the urine (10).

Recently, it has been shown that *in vitro* chronic treatment of podocytes with palmitic acid leads to insulin resistance in podocytes (11), which comprise the major constituent of the glomer-

* This work was supported by grants from the National Institute of Pharmaceutical Education and Research, S.A.S. Nagar, India and the Department of Science & Technology, Government of India. The authors declare that they have no conflicts of interest with the contents of this article.
◆ This article was selected as a Paper of the Week.
[S] This article contains supplemental Figs. 1 and 2.
[1] These authors contributed equally to this work.
[2] To whom correspondence should be addressed: Laboratory of Epigenetics and Diseases, Dept. of Pharmacology and Toxicology, National Institute of Pharmaceutical Education and Research (NIPER), Sector 67, S.A.S. Nagar, Punjab-160062, India. Tel.: 91-172-2292049; E-mail: tikoo.k@gmail.com.

ular filtration barrier. Podocyte injury is mainly characterized by effacement of its foot process and the loss of key molecules such as nephrin and podocin (12).

Metformin, a biguanide oral hypoglycemic agent, has been the drug of choice for type 2 diabetes for many years, reducing morbidity and mortality. There is a growing body of evidence suggesting pleiotropic effects of metformin. Apart from its glucose- and free fatty acid-lowering action by sensitizing insulin, it was shown by Piwkowska *et al.* (13) to activate AMP-activated protein kinase (AMPK)[3] and decrease NADPH oxidase (NOX) activity, thereby reducing reactive oxygen species production and TGF-β-induced epithelial-to-mesenchymal transition, a key event during the development of the tubulointerstitial fibrosis in diabetic nephropathy. Metformin reduces fat content by decreasing sterol regulatory element-binding protein 1 (SREBP-1), fatty acid synthetase (FAS), and acetyl-CoA carboxylase (ACC) expression in kidney (14).

Risk of kidney, eye, and nerve damage and nonfatal cardiovascular events can be reduced to almost ~50% only by following long-term intensive blood glucose control (15, 16). Because only long-term, intense blood glucose control (diet reversal) can reduce the risk of diabetic complications, there is a quest for a therapeutic agent that, along with intense blood glucose control, can harness the diet reversal within a short span of time (17). To achieve this objective, we used diet reversal along with metformin treatment for only 8 weeks to reverse the metabolic memory generated in 16 weeks.

Experimental Procedures

Animals—Adult male Sprague-Dawley rats of 180–200 g of body weight were procured from the Central Animal Facility, National Institute of Pharmaceutical Education and Research (NIPER), S.A.S. Nagar, India, and three rats/cage were housed under standard environmental conditions (temperature: 22 ± 2 °C; humidity: 50 ± 10%; and 12-h light/dark cycle) with access to food and water *ad libitum*. All protocols were approved by the Institutional Animal Ethics Committee (IAEC Approval Number 13/28, NIPER) and performed in accordance with the guidelines of the Committee for the Purpose of Control and Supervision of Experiments on Animals (CPCSEA), New Delhi, India.

Experimental Design—After 1 week of acclimatization, male Sprague-Dawley rats were randomly divided into two groups: CONTROL, which were fed with normal pellet diet (NPD), and HFD, which were fed with high fat diet (HFD). After 16 weeks, HFD-fed rats were further divided into three groups: (*a*) HFD-fed rats, which received HFD; (*b*) REV, which received NPD; and (*c*) REV+MET, which received NPD and metformin at 100 mg kg^{-1} day^{-1}, p.o. for a period of 8 weeks (supplemental Fig. 1*B*). Crushed/pelleted NPD feed was standard chow from Pranav Agro Industries, New Delhi, India. Lard was procured from a local slaughter house. HFD was prepared in-house as per the composition devised by Srinivasan *et al.* (18). Body weight was recorded every week right from the beginning to the end of the study. Blood biochemical parameters (glucose, lipid profile, and kidney function tests) were measured twice (8th and 16th weeks) during the insulin resistance model development (before diet reversal) and at the end (24th week) of the study (supplemental Fig. 1*A*).

Biochemical Parameters—After overnight fasting, blood was collected retro-orbitally under thiopentone anesthesia (50 mg kg^{-1}, i.p.), and then centrifuged at 4 °C, 2500 × *g* for 10 min for separation of plasma. Different biochemical parameters were estimated as per the manufacturer's guidelines (Accurex Biomedical Pvt. Ltd., Mumbai, India). The parameters measured were: glucose (GOD-POD); lipid profile: triglycerides (LPL-GK-GPO-POD); cholesterol (CHE-CHO-POD); kidney function tests (KFT): BUN (urease); and creatinine (Jaffe's initial rate method).

Hemodynamic Parameters—Invasive blood pressure and change in mean arterial pressure (ΔMAP) in response to bolus infusion of angiotensin II (200 ng kg^{-1}, i.v.) were measured as described earlier (19). Hemodynamic data were acquired and analyzed using LabChart 7 (ADInstruments, Bella Vista, New South Wales, Australia).

Western Blotting—Immunoblotting was performed as described earlier (20). Briefly, frozen kidneys were thawed, minced, and homogenized in lysis buffer containing surfactants and protease and phosphatase inhibitors. Protein samples were resolved using sodium dodecyl sulfate-polyacrylamide gels depending on the molecular weight of the desired proteins. These were then transferred to nitrocellulose membranes and were probed with primary and secondary antibodies, developed using an HRP-chemiluminescent substrate solution, and captured onto x-ray film, which was then scanned using a flatbed scanner to an 8-bit grayscale image. The intensity of the band in each lane was quantified using the ImageJ (National Institutes of Health) software. All antibodies were procured from Santa Cruz Biotechnology, Inc., unless otherwise specified. The antibodies were: phospho-AMPKα1/2 (sc-33524), AMPKα1/2 (sc-25792), tubulin (sc-23948), Cox-2 (sc-7951), IL-1β (sc-7884), caspase 3 (sc-7272), fibronectin (sc-9068, detects both cytoplasmic and extracellular fibronectin), α-SMA (sc-53015), and PARP (9542, Cell Signaling Technology).

Histopathology and Immunohistochemistry—Kidney was fixed in 10% v/v formal saline and embedded in paraffin, and 5-μm transverse sections were prepared and mounted on slides previously coated with poly-L-lysine and stained with hematoxylin and eosin (for glomerular space and glomerular tuft area) and picrosirius red (for extracellular matrix deposition). Coverslips were mounted and observed under OLYMPUS BX51 microscope. Immunostaining was performed for fibronectin and α-SMA on paraffin-embedded sections as described earlier (19).

TUNEL Assay—Terminal deoxynucleotidyl transferase-mediated dUTP nick end labeling (TUNEL) assay was performed on paraffin-embedded 5-μm-thick kidney sections to assess the DNA fragmentation. The assay was conducted according to the manufacturer's instructions. The images were

[3] The abbreviations used are: AMPK, AMP-activated protein kinase; PARP, poly(ADP-ribose) polymerase; ACC, acetyl-CoA carboxylase; α-SMA, α-smooth muscle actin; Ang II, angiotensin II; HFD, high fat diet; NPD, normal pellet diet; CHE-CHO-POD, cholesterol esterase-cholesterol oxidase-peroxidase; GOD-POD, glucose oxidase-peroxidase; LPL-GK-GPO-POD, lipoprotein lipase-glycerol kinase-glycerol phosphate oxidase-peroxidase; MAP, mean arterial pressure; ΔMAP, change in MAP; p.o., *per os* (orally); BUN, blood urea nitrogen; BW, body weight.

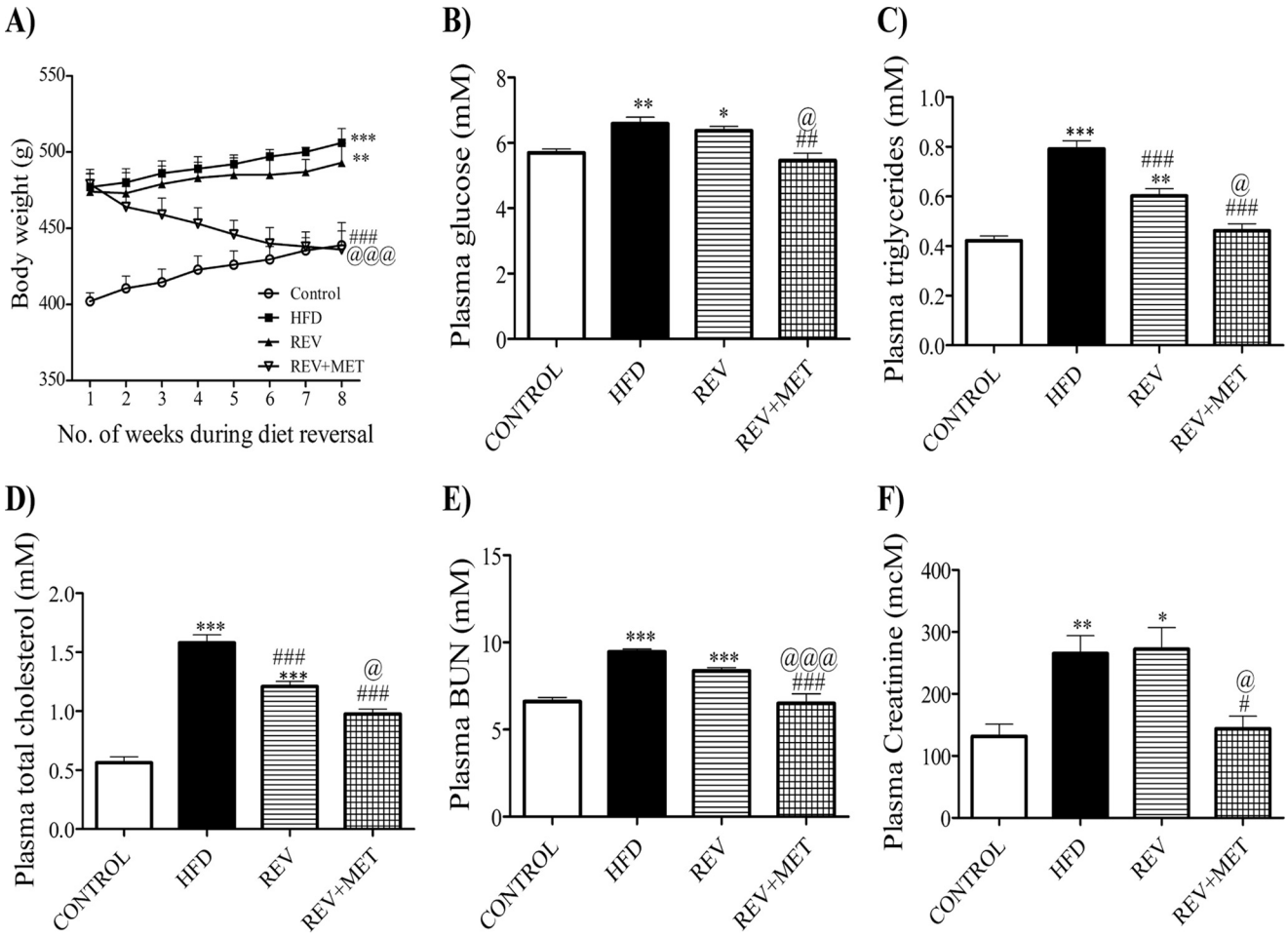

FIGURE 1. **Parameters after 8 weeks of diet reversal, *i.e.* from the 17th week to the 24th week of the study.** *A*, growth curve with body weights taken every week. *B–F*, glucose (*B*), triglycerides (*C*), cholesterol (*D*), blood urea nitrogen (*E*), and creatinine (*F*) measured at the end of the study after diet reversal. *CONTROL*, rats fed with normal pellet diet; *HFD*, rats fed with high fat diet; *REV*, reversal group rats fed with normal pellet diet for 8 weeks following 16 weeks of high fat diet feeding; *REV+MET*, reversal group rats fed with normal pellet diet and treated with metformin (100 mg kg^{-1} day^{-1}, p.o.) after 16 weeks of high fat diet feeding. *, $p < 0.05$, **, $p < 0.01$, ***, $p < 0.001$ *versus* CONTROL; #, $p < 0.05$, ##, $p < 0.01$, ###, $p < 0.001$ *versus* HFD; @, $p < 0.05$, @@@, $p < 0.001$ *versus* REV; $n = 6$.

TABLE 1

Morphometric and hemodynamic parameters

Initial BW was taken after the 16-week period, *i.e.* at the 17th week, and final BW was taken on the day of sacrifice. CONTROL, control rats fed with normal pellet diet; HFD, rats fed with high fat diet throughout the study for 24 weeks; REV, rats fed with high fat diet for 16 weeks and switched to normal diet for the next 8 weeks; REV+MET, rats fed with high fat diet for 16 weeks and switched to normal diet and treated with metformin (100 mg kg^{-1} day^{-1}, p.o.) for the next 8 weeks. BW, body weight; KW, kidney weight; HW, heart weight; LW, liver weight; WAT, white adipose tissue; MAP, mean arterial pressure; ΔMAP, acute change of MAP in response to a bolus of angiotensin II (200 ng kg^{-1}). *, $p < 0.05$, **, $p < 0.01$, and ***, $p < 0.001$ *versus* control; #, $p < 0.05$, ##, $p < 0.01$, and ###, $p < 0.001$ versus HFD; @, $p < 0.05$, @@, $p < 0.01$, and @@@, $p < 0.001$ *versus* REV, $n = 6$.

Parameter	CONTROL	HFD	REV	REV+MET
Initial BW (g)	402.08 ± 5.24	473.55 ± 8.74***	469.45 ± 11.20***	472.75 ± 10.94***
Final BW (g)	438.8 ± 8.92	506.22 ± 4.79***	493.91 ± 11.04***	438.4 ± 11.98##,@@
Absolute kidney weight (g)	2.40±.07	2.93 ± 0.18**	2.83 ± 0.05**	2.54 ± 0.05#,@
KW/BW (mg g^{-1})	5.19 ± 0.09	5.83 ± 0.04**	5.79 ± 0.03**	5.38 ± 0.06##,@@
KW/tibial length (g cm^{-1})	0.57 ± 0.02	0.70 ± 0.03**	0.68 ± 0.02**	0.60 ± 0.01#,@
Absolute heart weight (g)	1.17 ± 0.02	1.31 ± 0.02**	1.30 ± 0.013**	1.20 ± 0.008#,@
HW/BW (mg g^{-1})	2.52 ± 0.07	2.89 ± 0.06**	2.90 ± 0.05**	2.57 ± 0.07#,@
HW/tibial length (g cm^{-1})	0.28 ± 0.005	0.32 ± 0.003***	0.32 ± 0.004***	0.29 ± 0.007##,@@
Absolute liver weight (g)	13.25 ± 0.48	18.47 ± 0.57***	16.97 ± 0.30***	12.99 ± 0.79###,@@@
LW/BW (mg g^{-1})	27.56 ± 1.25	36.12 ± 0.98***	34.14 ± 0.31**	27.70 ± 1.76###,@@
WAT (g)	6.55 ± 0.77	12.94 ± 0.64***	12.06 ± 0.10***	7.88 ± 0.98##,@
WAT/BW (mg g^{-1})	13.54 ± 1.32	28.83 ± 1.58***	28.58 ± 3.04***	16.00 ± 2.80##,@@
MAP (mmHg)	82.74 ± 2.33	98.24 ± 1.30**	93.42 ± 1.30*	83.37 ± 0.50##@
ΔMAP in response to Ang II 200 mg kg^{-1}	23.78 ± 1.27	35.08 ± 0.97**	32.87 ± 2.70*	25.14 ± 0.16##@

acquired using a charge-coupled device (CCD) camera. Finally, the average number of TUNEL-positive apoptotic bodies per glomerulus was calculated.

Statistical Analysis—All the data were expressed as mean ± S.E. Means of two groups were compared using unpaired Student's *t* test, and means of multiple groups were com-

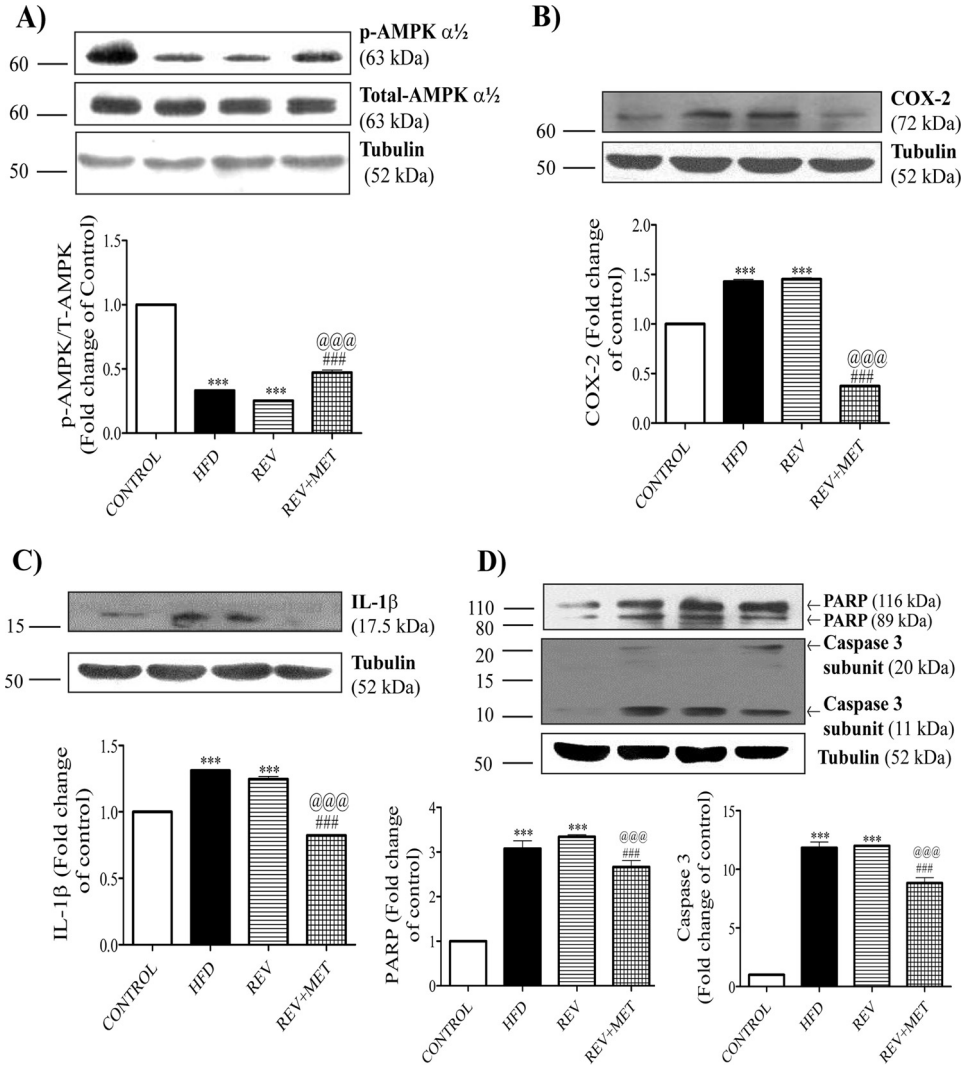

FIGURE 2. **Western blots of whole kidney lysates.** 60 μg of protein was loaded per each lane. 8, 10, and 12% SDS-PAGE gels were run according to the molecular weight of the protein of interest. To ensure the correct position of the protein of interest, a pre-stained protein marker (Invitrogen Novex® Sharp Pre-stained Protein Standard, catalog number LC5800, Thermo Fisher Scientific) was run along with the samples. Tubulin was used as internal control for normalization, and results are expressed as -fold change over control rats. *A*, Western blots and quantification for phospho-AMPK (*p-AMPK*), total AMPK, and tubulin. *B*, Western blots and quantification for inflammatory markers: COX-2 and tubulin. *C*, Western blots and quantification for inflammatory cytokines: IL-1β and tubulin. *D*, Western blots and quantifications for apoptotic markers: PARP, caspase 3, and tubulin. *CONTROL*, rats fed with normal pellet diet; *HFD*, rats fed with high fat diet; *REV*, reversal group rats fed with normal pellet diet for 8 weeks following 16 weeks of high fat diet feeding; *REV+MET*, reversal group rats fed with normal pellet diet and treated with metformin (100 mg kg^{-1} day^{-1}, p.o.) after 16 weeks of high fat diet feeding. $n = 3$ blots. ***, $p < 0.001$ *versus* CONTROL; ###, $p < 0.001$ *versus* HFD; @@@, $p < 0.001$ *versus* REV.

pared using analysis of variance followed by Bonferroni's post hoc test. Values were considered statistically significant if $p < 0.05$. The statistical software used for analyzing the data was GraphPad Prism, version 5.01 (GraphPad Software, Inc.).

Results

High Fat Diet Feeding Induces Insulin Resistance—In accordance with earlier studies (19, 21), high fat diet-fed animals in our study exhibited significant increase in body weight, plasma glucose, triglycerides, and cholesterol levels at 8, 16, and 24 weeks of high fat diet feeding (supplemental Fig. 2). The higher rate of body weight gain was accentuated from 6 weeks onwards in HFD-fed rats. These results indicate the development of insulin resistance under hyperlipidemic conditions (elevated levels of circulating saturated free fatty acids) was reached after feeding high fat diet.

Short-term Diet Reversal Displays Metabolic Memory, and Metformin Attenuates Metabolic Memory—The body weight gain of the reversal group was comparable with that of HFD even after 8 weeks of diet reversal, suggesting the footprints of the earlier poor glycemic control (high fat diet) period. Metformin was found to be effective in reducing the body weight gain from the first week of treatment itself (Fig. 1*A*). Diet reversal could not affect the hyperglycemia induced by high fat diet, indicating the presence of metabolic memory (Fig. 1*B*). However, metformin attenuated the elevated glucose, triglycerides, and cholesterol (Fig. 1, *B–D*).

Kidney Function Parameters—Plasma blood urea nitrogen and plasma creatinine rose from the 16th week of high fat diet

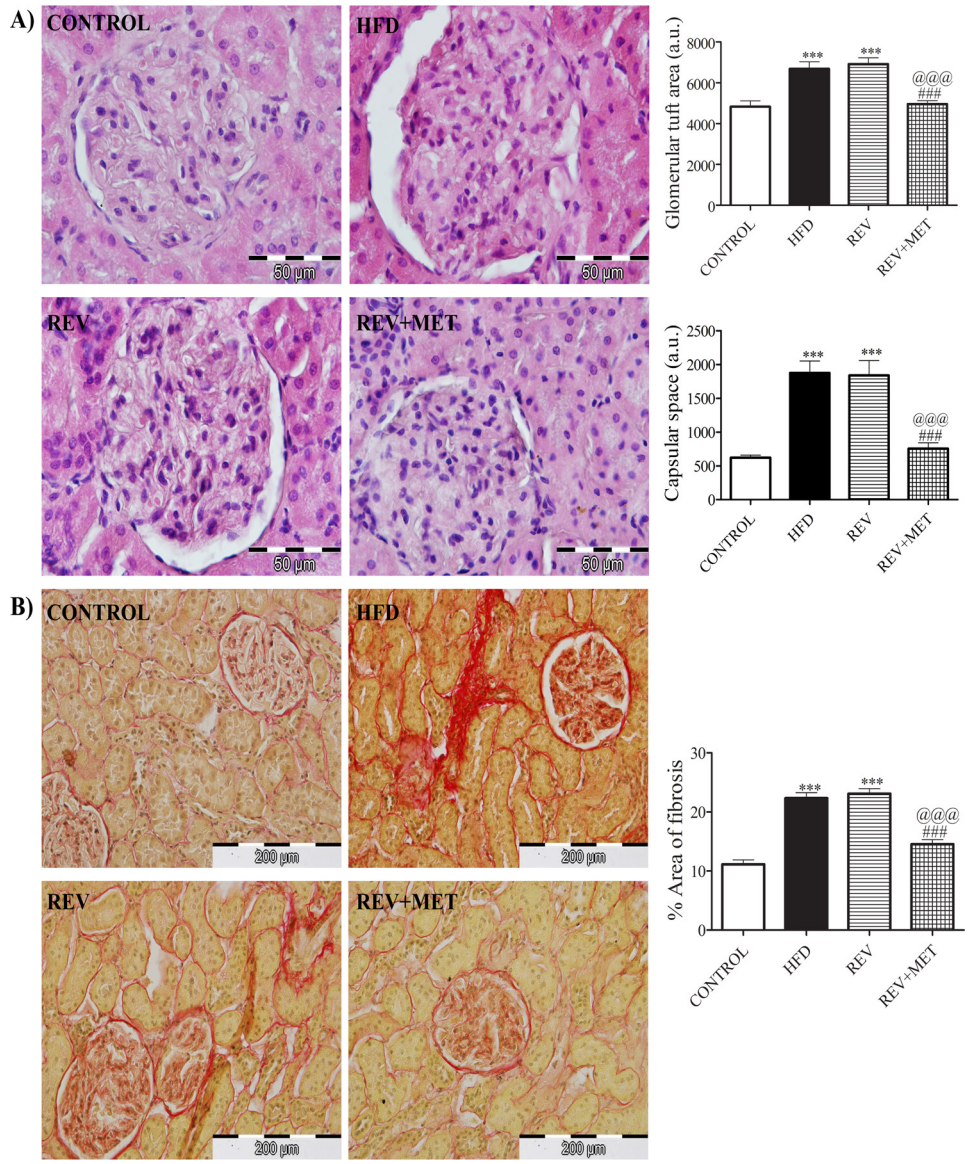

FIGURE 3. **H&E and picrosirius red staining of kidney.** *A*, H&E-stained images under 1000× magnification along with quantification of glomerular tuft area and capsular space. *B*, picrosirius red-stained images showing glomerular fibrosis under 400× magnification along with quantification of interstitial fibrosis. *CONTROL*, rats fed with normal pellet diet; *HFD*, rats fed with high fat diet; *REV*, reversal group rats fed with normal pellet diet for 8 weeks following 16 weeks of high fat diet feeding; *REV+MET*, reversal group rats fed with normal pellet diet and treated with metformin (100 mg kg^{-1} day^{-1}, p.o.) after 16 weeks of high fat diet feeding. $n = 10–12$ sections from each group. ***, $p < 0.001$ *versus* CONTROL; ###, $p < 0.001$ *versus* HFD; @@@, $p < 0.001$ *versus* REV.

feeding, indicating the development of renal dysfunction. Diet switching did not improve the renal function indicators. However, metformin improved renal dysfunction by decreasing the plasma urea and creatinine levels (Fig. 1, *E* and *F*).

Metformin Improves Cardiovascular Function—It has been postulated that elevated basal MAP exacerbates nephropathy (22). To investigate this phenomenon, invasive blood pressure was measured in our study. HFD-fed rats had significantly higher basal MAP and increased response (change in MAP) to angiotensin II at a dose of 200 ng kg^{-1} as compared with age-matched control rats. Diet reversal failed to restore both hemodynamic parameters. Metformin lowered the basal MAP as well as the Ang II-mediated change in MAP, comparable with the control group (Table 1).

Metformin Activates AMPK—High fat diet significantly reduced the level of activated AMPK, and diet reversal could not restore it. We found that none of the diet/treatment manipulations changed the basal levels of AMPK. Metformin, a known AMPK activator (23), increased the activity of AMPK, as evident from the increased levels of the phosphorylated form of AMPK in Western blotting (Fig. 2*A*).

Metformin Reduces Renal Inflammation, Apoptosis, and Fibrosis—Clinical and experimental studies highlighted the association of high fat diet with inflammation and apoptosis (24, 25). Hence, we also checked the molecular markers of renal inflammation, apoptosis, and fibrosis. High fat diet feeding significantly augmented the levels of COX-2, a non-steroidal anti-inflammatory drug-sensitive pathological inflammation-mediating enzyme, and IL-1β, an inflammatory cytokine (Fig. 2, *B* and *C*). HFD feeding also instigated apoptosis in kidney, as evident from the surge in the proapoptotic caspase 3 and PARP, an enzyme involved in DNA repair (Fig. 2*D*), and also the

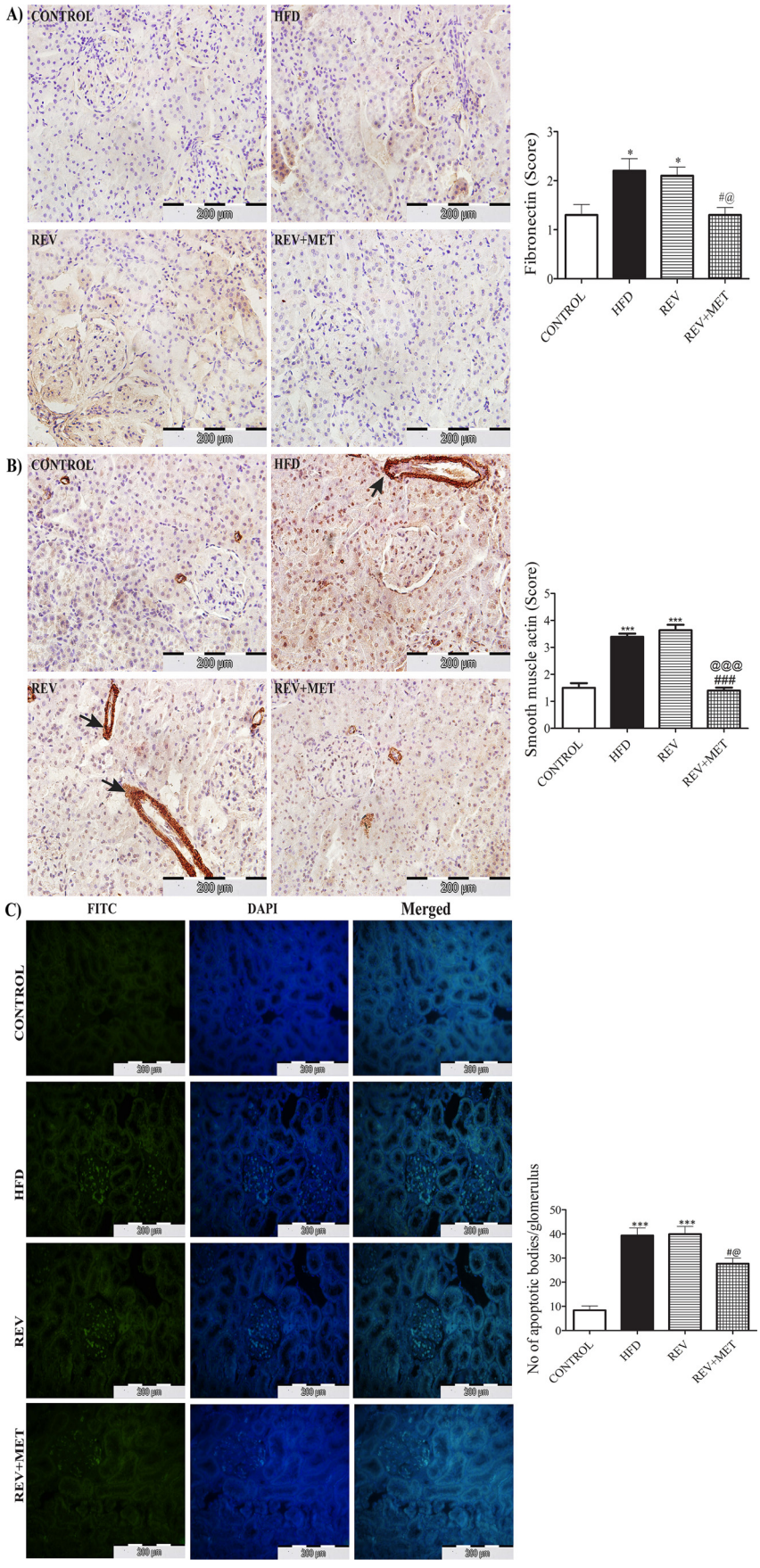
A)
CONTROL
HFD
REV
REV+MET
200 μm
Fibronectin (Score)
CONTROL
HFD
REV
REV+MET
B)
CONTROL
HFD
REV
REV+MET
200 μm
Smooth muscle actin (Score)
CONTROL
HFD
REV
REV+MET
C)
FITC
DAPI
Merged
CONTROL
HFD
REV
REV+MET
300 μm
No of apoptotic bodies/glomerulus
CONTROL
HFD
REV
REV+MET

increased number of apoptotic bodies as observed by TUNEL assay (see Fig. 4*C*). Diet reversal was unable to improve the renal inflammation and apoptosis, emphasizing the persistence of renal injury even after 8 weeks of dietary control. However, metformin treatment was able to reduce the levels of inflammatory and apoptotic markers.

Collagen and fibronectin are key components of the extracellular matrix during sclerosis (scar formation) following an episode of inflammatory injury in a tissue as a part of tissue repair (26). Interestingly, high fat diet also increased the deposition of α-SMA and fibronectin in the kidney, as evident from the immunostaining. Diet reversal could not bring down the levels of fibronectin and α-SMA, but metformin demonstrated its ability to ameliorate renal fibrosis (see Fig. 4, *A* and *B*). Kidney weight, both *per se* and when normalized with body weight or tibial length, crude markers of hypertrophy, increased significantly in animals fed with high fat diet, which could not be assuaged by switching to normal diet but could be normalized when treated with metformin (Table 1).

Metformin Ameliorates Insulin Resistance-induced Gross Morphological and Microscopic Histological Changes—High fat diet significantly amplified body weight gain and white adiposity index, indicating the presence of obesity. It also increased the weights of kidney, heart, and liver, either when considered alone or even after normalization with tibial length (Table 1). The latter is an excellent index of hypertrophy. Tibial length, but not body weight, is recommended as an index of hypertrophy of an organ, especially in cases where the body weight changes as in the case of obesity (27). Diet reversal proved inefficient in encountering the aberrations induced by HFD feeding, but diet reversal in combination with metformin could suppress them (Table 1).

Histological cross-sections of HFD-fed kidney observed under a microscope showed increased glomerular size (glomerular tuft area) and glomerular space as revealed by H&E staining (Fig. 3*A*), as well as collagenous extracellular matrix (tubulointerstitial fibrosis) as revealed by picrosirius red staining (Fig. 3*B*). These aberrations caused by HFD were not alleviated by diet reversal alone but could be achieved in combination with metformin.

Discussion

We provide the first evidence that metformin prevents the metabolic memory responsible for the progression of HFD-induced renal dysfunction. Previously, we have reported the presence of metabolic memory in renal and vascular endothelial dysfunction induced by HFD (21, 28). Feeding rats with high fat diet for 16 weeks induced insulin resistance characterized by elevated blood glucose, triglycerides, and cholesterol, in agreement with the previous results of our lab (29, 30). Elevated plasma BUN and creatinine showed the development of renal dysfunction after 16 weeks of HFD feeding. Subsequent diet reversal for 8 weeks reduced lipid levels but could not mitigate hyperglycemia and renal dysfunction. However, metformin treatment (100 mg kg^{-1} day^{-1}) along with diet reversal effectively restored insulin sensitivity and renal function.

Our model mimics the clinical situation in which high calorie/high fat diet induces renal complications in insulin resistance conditions. It is an early stage nephropathy because there was no change in the plasma levels of albumin (data not shown). The initial exposure to hyperglycemia and hypertriglyceridemia prevented the high fat-fed animals from responding to diet reversal at the biochemical, molecular, microscopic, and macroscopic levels, indicating the development of metabolic memory in our model. Here we show that 8 weeks of diet reversal, after 16 weeks of high fat diet feeding, could not restore the aberrations of insulin resistance, but diet reversal along with metformin treatment for a short duration (8 weeks) shows remarkable amelioration of anomalies associated with insulin resistance. Metformin treatment prevents HFD-induced metabolic memory and reverses renal complications.

Clinically, it has been shown that insulin resistance and hypertension are major contributors of renal dysfunction (22). In line with the above study, in our animal model, invasive blood pressure measurement showed an increase in MAP and Ang II-induced ΔMAP, which could not be reversed upon diet reversal. Metformin has been reported to have an anti-hypertensive effect in diabetes (31). Our study also found that metformin significantly mitigated the basal as well as the Ang II-induced MAP elevation. Enhanced angiotensin II induced acute contractile responses, and worsened endothelial dependent vasodilation in HFD-fed rats *ex vivo* has been shown to be associated with down-regulation of SIRT1/AMPK/eNOS (endothelial NOS) pathway (19, 29), suggesting to us that the improvement in hemodynamic parameters observed during metformin treatment may also involve up-regulation of this pathway.

AMPK is the master sensor of cellular energy metabolism and is initially activated during metabolic stress conditions (impaired ATP production and excess ATP consumption) such as diabetes and obesity, but is inhibited as the disease progresses (32). AMPK is suppressed in various organs, including kidney in high fat consumption, and its activation by 5-amino-4-imidazole carboxamide riboside (AICAR) or metformin was shown to be effective in reversing renal damage (33, 34). In line with this result, we observed a significant fall in the activity of renal AMPK in high fat-fed rats. Diet reversal could not restore the activity of AMPK unless combined with metformin treatment. AMPK activation inhibits inflammation in MRL/lpr

FIGURE 4. **Immunohistochemistry of renal fibronectin, α-SMA, and TUNEL assay in kidney sections.** *A* and *B*, 3,3′-diaminobenzidine-stained images of fibronectin and α-SMA under 400× magnification (*A*) and quantification of immunohistochemistry by the indicated scoring method (*B*). Scores were measured as follows: 1 = no or very low color, 2 = mild color, 3 = moderate color, 4 = intense brown color. *Arrows* indicate the extracellular areas of α-SMA immunostaining. *C*, FITC and DAPI staining and merged images of TUNEL assay under 400× magnification along with quantification of apoptotic bodies/glomerulus. *CONTROL*, rats fed with normal pellet diet; *HFD*, rats fed with high fat diet; *REV*, reversal group rats fed with normal pellet diet for 8 weeks following 16 weeks of high fat diet feeding; *REV*+*MET*, reversal group rats fed with normal pellet diet and treated with metformin (100 mg kg^{-1} day^{-1}, p.o.) after 16 weeks of high fat diet feeding. $n = 10–12$ sections from each group. *, $p < 0.05$ and ***, $p < 0.001$ *versus* CONTROL; #, $p < 0.05$, ###, $p < 0.001$ *versus* HFD; @, $p < 0.05$, @@@, $p < 0.001$ *versus* REV.

mouse mesangial cells and *in vivo* renal inflammation by decreasing MCP-1 (33, 35). In our study, renal COX-2 and IL-1β, the markers of inflammation, were repressed by metformin, but not by diet reversal alone.

The beneficial effect of metformin treatment in reversing metabolic memory in a short duration (8 weeks) can be explained if we assume that metformin increases renal fatty acid oxidation by modulating AMPK/ACC pathway and in turn reducing renal lipotoxicity. ACC is a rate-limiting enzyme required for the generation of malonyl-coenzyme A (malonyl-CoA), which plays a critical role in the synthesis of fatty acids and inhibition of mitochondrial fatty acid oxidation. AMPK inhibits this ACC by phosphorylating it (34).

At the macroscopic level, the kidney index significantly increased in the HFD group and decreased only when subjected to diet reversal and metformin treatment. Crinigan *et al.* (36) has shown significant increase in the renal mass of Sprague-Dawley rats just after 6 weeks of high fat diet feeding. In addition, other studies have also shown that high fat diet feeding increases kidney weight (37, 38).

Histological sections of kidney showed characteristic structural alteration by HFD feeding, such as increased glomerular size and Bowman's capsular space as reported earlier (25). We also observed similar microscopic maladaptations in kidney even after diet reversal. During tissue repair and wound healing, the differentiation of tubular epithelial and progenitor cells, vascular pericytes and endothelial cells, and interstitial cells such as fibroblasts into myofibroblasts results in the deposition of extracellular matrix components such as collagen and fibronectin. However, excess deposition of extracellular matrix results in fibrosis. α-SMA is a selective marker of myofibroblasts (39). In our present study, collagen, fibronectin, and α-SMA increased in the HFD group and were attenuated only after treatment with metformin along with high fat diet reversal. Microscopic examination of kidney sections using picrosirius staining revealed the extent of renal injury as observed in terms of glomerular and interstitial fibrosis. The extent of renal damage after initial high fat consumption was comparable in both groups (HFD and REV), indicating no potential benefit of diet reversal. Metformin, an AMPK activator, significantly improved renal fibrosis. The immunohistochemical scores of fibronectin and α-SMA also confirmed the same results (Fig. 4). AMPK plays a crucial role in maintaining the structural integrity of kidney. AMPK activation by metformin restored the normal structure and physiology of kidney. Inhibition of AMPK has been reported to be associated with increased profibrotic markers (40). The decreased level of the phosphorylated form of AMPK coincided with increased collagen and extracellular matrix deposition in kidney of HFD-fed animals and its reversal by metformin treatment. This can very well explain the protection observed by metformin treatment but not by diet reversal.

Insulin resistance induces podocyte death, modulating the phosphorylation of PP2A and mTORc1 (41). High fat-mediated insulin resistance showed an increase in renal cell death and apoptotic bodies, which was confirmed with the increased protein expression of the apoptosis markers, PARP and caspase 3. Metformin effectively reduced renal apoptosis, as evident from the reduced number of TUNEL-positive cells.

Our data enable us to conclude that due to metabolic memory, short-term diet reversal cannot reverse the insulin resistance-induced complications. However, complications due to metabolic memory can very well be prevented by metformin, an AMPK activator. Recently, we have shown that fatty acid/high fat diet-induced metabolic memory involves changes in renal histone H3K36me2 and H3K27me3 (28). Further studies are required to ascertain the role of metformin in epigenetic alterations responsible for preventing metabolic memory.

Author Contributions—K. T. conceived the idea, designed and supervised the study, and approved the manuscript. E. S. prepared the high fat diet, treated animals, did biochemical and histological experiments and Western blotting, and wrote manuscript. V. R. A. performed hemodynamic experiments, histological experiments, and Western blotting and wrote manuscript. H. P. and V. S. D. helped during experiments.

Acknowledgments—We are grateful to Umashanker Navik for providing selfless help in capturing and quantification of histological images. We owe a lot to Pinakin Arun Karpe and Sandeep Kumar of our lab for their insightful discussion.

Note Added in Proof—In the version of this paper that was published as a Paper in Press on August 22, 2016, an incorrect figure was uploaded as Fig. 1. Additionally, Fig. 4*C* was labeled incorrectly. Errors arose while incorporating the figure/label in the manuscript. These errors have now been corrected and do not affect the results or conclusions of this work.

References

1. Tonna, S., El-Osta, A., Cooper, M. E., and Tikellis, C. (2010) Metabolic memory and diabetic nephropathy: potential role for epigenetic mechanisms. *Nat. Rev. Nephrol.* **6,** 332–341
2. Zick, Y. (2003) Role of Ser/Thr kinases in the uncoupling of insulin signaling. *Int. J. Obes. Relat. Metab. Disord.* **27,** Suppl. 3, S56–S60
3. Villeneuve, L. M., and Natarajan, R. (2010) The role of epigenetics in the pathology of diabetic complications. *Am. J. Physiol. Renal Physiol.* **299,** F14–F25
4. Drzewoski, J., Kasznicki, J., and Trojanowski, Z. (2009) The role of "metabolic memory" in the natural history of diabetes mellitus. *Pol. Arch. Med. Wewn.* **119,** 493–500
5. Zick, Y. (2004) Uncoupling insulin signalling by serine/threonine phosphorylation: a molecular basis for insulin resistance. *Biochem. Soc. Trans.* **32,** 812–816
6. Randle, P. J., Garland, P. B., Newsholme, E. A., and Hales, C. N. (1965) The glucose fatty acid cycle in obesity and maturity onset diabetes mellitus. *Ann. N.Y. Acad. Sci.* **131,** 324–333
7. Shulman, G. I. (2000) Cellular mechanisms of insulin resistance. *J. Clin. Invest.* **106,** 171–176
8. Roden, M., Price, T. B., Perseghin, G., Petersen, K. F., Rothman, D. L., Cline, G. W., and Shulman, G. I. (1996) Mechanism of free fatty acid-induced insulin resistance in humans. *J. Clin. Invest.* **97,** 2859–2865
9. Yang, J., Park, Y., Zhang, H., Xu, X., Laine, G. A., Dellsperger, K. C., and Zhang, C. (2009) Feed-forward signaling of TNF-α and NF-κB via IKK-β pathway contributes to insulin resistance and coronary arteriolar dysfunction in type 2 diabetic mice. *Am. J. Physiol. Heart Circ. Physiol.* **296,** H1850–H1858
10. Peng, J., Li, X., Feng, Q., Chen, L., Xu, L., and Hu, Y. (2013) Anti-fibrotic effect of *Cordyceps sinensis* polysaccharide: inhibiting HSC activation, TGF-β1/Smad signalling, MMPs and TIMPs. *Exp. Biol. Med. (Maywood)* **238,** 668–677
11. Lennon, R., Pons, D., Sabin, M. A., Wei, C., Shield, J. P., Coward, R. J., Tavaré, J. M., Mathieson, P. W., Saleem, M. A., and Welsh, G. I. (2009)

Saturated fatty acids induce insulin resistance in human podocytes: implications for diabetic nephropathy. *Nephrol. Dial. Transplant.* **24,** 3288–3296
12. Deegens, J. K. J., Dijkman, H. B. P. M., Borm, G. F., Steenbergen, E. J., van den Berg, J. G., Weening, J. J., and Wetzels, J. F. M. (2008) Podocyte foot process effacement as a diagnostic tool in focal segmental glomerulosclerosis. *Kidney Int.* **74,** 1568–1576
13. Piwkowska, A., Rogacka, D., Jankowski, M., Dominiczak, M. H., Stepiński, J. K., and Angielski, S. (2010) Metformin induces suppression of NAD(P)H oxidase activity in podocytes. *Biochem. Biophys. Res. Commun.* **393,** 268–273
14. Wang, W., Guo, X. H., Wu, H. H., Wang, N. H., and Xu, X. S. (2006) [Effect of fenofibrate and metformin on lipotoxicity in OLETF rat kidney]. *Beijing Da Xue Xue Bao* **38,** 170–175
15. The Diabetes Control and Complications Trial Research Group (1993) The effect of intensive treatment of diabetes on the development and progression of long-term complications in insulin-dependent diabetes mellitus. *N. Engl. J. Med.* **329,** 977–986
16. Nathan, D. M., Cleary, P. A., Backlund, J. Y., Genuth, S. M., Lachin, J. M., Orchard, T. J., Raskin, P., and Zinman, B.; Diabetes Control and Complications Trial/Epidemiology of Diabetes Interventions and Complications (DCCT/EDIC) Study Research Group (2005) Intensive diabetes treatment and cardiovascular disease in patients with type 1 diabetes. *N. Engl. J. Med.* **353,** 2643–2653
17. Zhang, L., Chen, B., and Tang, L. (2012) Metabolic memory: mechanisms and implications for diabetic retinopathy. *Diabetes Res. Clin. Pract.* **96,** 286–293
18. Srinivasan, K., Patole, P. S., Kaul, C. L., and Ramarao, P. (2004) Reversal of glucose intolerance by pioglitazone in high fat diet-fed rats. *Methods Find. Exp. Clin. Pharmacol.* **26,** 327–333
19. Karpe, P. A., and Tikoo, K. (2014) Heat shock prevents insulin resistance-induced vascular complications by augmenting angiotensin-(1–7) signaling. *Diabetes* **63,** 1124–1139
20. Tikoo, K., Bhatt, D. K., Gaikwad, A. B., Sharma, V., and Kabra, D. G. (2007) Differential effects of tannic acid on cisplatin induced nephrotoxicity in rats. *FEBS Lett.* **581,** 2027–2035
21. Tallapragada, D. S., Karpe, P. A., and Tikoo, K. (2015) Long-lasting partnership between insulin resistance and endothelial dysfunction: role of metabolic memory. *Br. J. Pharmacol.* **172,** 4012–4023
22. El-Atat, F. A., Stas, S. N., McFarlane, S. I., and Sowers, J. R. (2004) The relationship between hyperinsulinemia, hypertension and progressive renal disease. *J. Am. Soc. Nephrol.* **15,** 2816–2827
23. Meng, S., Cao, J., He, Q., Xiong, L., Chang, E., Radovick, S., Wondisford, F. E., and He, L. (2015) Metformin activates AMP-activated protein kinase by promoting formation of the $\alpha\beta\gamma$ heterotrimeric complex. *J. Biol. Chem.* **290,** 3793–3802
24. Wu, Y., Liu, Z., Xiang, Z., Zeng, C., Chen, Z., Ma, X., and Li, L. (2006) Obesity-related glomerulopathy: insights from gene expression profiles of the glomeruli derived from renal biopsy samples. *Endocrinology* **147,** 44–50
25. Deji, N., Kume, S., Araki, S., Soumura, M., Sugimoto, T., Isshiki, K., Chin-Kanasaki, M., Sakaguchi, M., Koya, D., Haneda, M., Kashiwagi, A., and Uzu, T. (2009) Structural and functional changes in the kidneys of high-fat diet-induced obese mice. *Am. J. Physiol. Renal Physiol.* **296,** F118–F126
26. Sawicka, K. M., Seeliger, M., Musaev, T., Macri, L. K., and Clark, R. A. (2015) Fibronectin interaction and enhancement of growth factors: importance for wound healing. *Adv. Wound Care (New Rochelle)* **4,** 469–478
27. Yin, F. C., Spurgeon, H. A., Rakusan, K., Weisfeldt, M. L., and Lakatta, E. G. (1982) Use of tibial length to quantify cardiac hypertrophy: application in the aging rat. *Am. J. Physiol.* **243,** H941–H947
28. Kumar, S., Pamulapati, H., and Tikoo, K. (2016) Fatty acid induced metabolic memory involves alterations in renal histone H3K36me2 and H3K27me3. *Mol. Cell. Endocrinol.* **422,** 233–242
29. Bendale, D. S., Karpe, P. A., Chhabra, R., Shete, S. P., Shah, H., and Tikoo, K. (2013) 17-β Oestradiol prevents cardiovascular dysfunction in postmenopausal metabolic syndrome by affecting SIRT1/AMPK/H3 acetylation. *Br. J. Pharmacol.* **170,** 779–795
30. Karpe, P. A., Gupta, J., Marthong, R. F., Ramarao, P., and Tikoo, K. (2012) Insulin resistance induces a segmental difference in thoracic and abdominal aorta: differential expression of AT1 and AT2 receptors. *J. Hypertens.* **30,** 132–146
31. Majithiya, J. B., and Balaraman, R. (2006) Metformin reduces blood pressure and restores endothelial function in aorta of streptozotocin-induced diabetic rats. *Life Sci.* **78,** 2615–2624
32. Towler, M. C., and Hardie, D. G. (2007) AMP-activated protein kinase in metabolic control and insulin signaling. *Circ. Res.* **100,** 328–341
33. Declèves, A. E., Mathew, A. V., Cunard, R., and Sharma, K. (2011) AMPK mediates the initiation of kidney disease induced by a high-fat diet. *J. Am. Soc. Nephrol.* **22,** 1846–1855
34. Kim, D., Lee, J. E., Jung, Y. J., Lee, A. S., Lee, S., Park, S. K., Kim, S. H., Park, B. H., Kim, W., and Kang, K. P. (2013) Metformin decreases high-fat diet-induced renal injury by regulating the expression of adipokines and the renal AMP-activated protein kinase/acetyl-CoA carboxylase pathway in mice. *Int. J. Mol. Med.* **32,** 1293–1302
35. Peairs, A., Radjavi, A., Davis, S., Li, L., Ahmed, A., Giri, S., and Reilly, C. M. (2009) Activation of AMPK inhibits inflammation in MRL/lpr mouse mesangial cells. *Clin. Exp. Immunol.* **156,** 542–551
36. Crinigan, C., Calhoun, M., and Sweazea, K. L. (2015) Short-term high fat intake does not significantly alter markers of renal function or inflammation in young male Sprague-Dawley rats. *J. Nutr. Metab.* **2015,** 157520
37. Nayak, B. K., Shanmugasundaram, K., Friedrichs, W. E., Cavaglierii, R. C., Patel, M., Barnes, J., and Block, K. (2016) HIF-1 mediates renal fibrosis in OVE26 type 1 diabetic mice. *Diabetes* **65,** 1387–1397
38. Shevalye, H., Lupachyk, S., Watcho, P., Stavniichuk, R., Khazim, K., Abboud, H. E., and Obrosova, I. G. (2012) Prediabetic nephropathy as an early consequence of the high-calorie/high-fat diet: relation to oxidative stress. *Endocrinology* **153,** 1152–1161
39. Grande, M. T., and López-Novoa, J. M. (2009) Fibroblast activation and myofibroblast generation in obstructive nephropathy. *Nat. Rev. Nephrol.* **5,** 319–328
40. Kume, S., Uzu, T., Araki, S., Sugimoto, T., Isshiki, K., Chin-Kanasaki, M., Sakaguchi, M., Kubota, N., Terauchi, Y., Kadowaki, T., Haneda, M., Kashiwagi, A., and Koya, D. (2007) Role of altered renal lipid metabolism in the development of renal injury induced by a high-fat diet. *J. Am. Soc. Nephrol.* **18,** 2715–2723
41. Kumar, S., and Tikoo, K. (2015) Independent role of PP2A and mTORc1 in palmitate induced podocyte death. *Biochimie* **112,** 73–84